



Discovery of a common light chain bispecific antibody targeting PD-1 and PD-L1 by Hybridoma-to-Phage-to-Yeast (H2PtY) platform

Peipei Liu, Chunyin Gu, Xiaodan Cao, Huawei Zhang, Zongda Wang, Yukun Yang , KeDong OuYang, Yingying Zhen, Fangfang Jia, Xianqing He, Haixiang Yu^{†,*}, Sujun Deng ^{†,*}

Biologics Innovation Institute, Shanghai Jemincare Pharmaceutical Co., Ltd., Lane 535, Huanqiao Road, Pudong New Area, Shanghai 201315, China

*Corresponding authors. Sujun Deng, Biologics Innovation Institute, Shanghai Jemincare Pharmaceutical Co., Ltd., Lane 535, Huanqiao Road, Pudong New Area, Shanghai 201315, China. E-mail: sujun@yahoo.com; Haixiang Yu, Biologics Innovation Institute, Shanghai Jemincare Pharmaceutical Co., Ltd., Lane 535, Huanqiao Road, Pudong New Area, Shanghai 201315, China. E-mail: yuhaixiang@jemincare.com

[†]Sujun Deng and Haixiang Yu are co-corresponding authors.

Abstract

Background: Therapeutic antibody drugs targeting the PD-1 pathway are generally characterized by relatively low response rates and susceptibility to drug resistance during clinical application. Therefore, there is an urgent need for alternative therapeutic strategies to increase the immune response rate. Bispecific antibodies co-targeting PD-1 and PD-L1 may have greater potential to improve the efficacy of the immune checkpoint pathway.

Method: In this study, we developed a potent humanized common light chain (CLC) IgG shape bispecific antibody (bsAb), named JMB2005, based on Hybridoma-to-Phage-to-Yeast platform. The platform allowed us to discover CLC bsAb from traditional mice for any pair of given targets.

Results: JMB2005 exhibited favorable developability, good manufacturing property, and satisfactory efficacy, which could be given via subcutaneous injection at the concentration of 120 mg/mL. Mechanistically, JMB2005 could bridge tumor cells and T cells with both Fab arms and promote T-cells to function as direct tumor cell killers. It could also promote T cell activation by blocking the binding of PD-L1 to CD80. Furthermore, JMB2005 has exhibited a favorable half-life and has demonstrated promising anti-tumor therapeutic efficacy *in vivo*.

Conclusion: Consequently, the present study showed that the novel humanized CLC bsAb JMB2005 may represent a novel therapeutic agent of great clinical potential.

Statement of Significance: We discovered a common light chain (CLC) bispecific antibody targeting PD-1 and PD-L1 with favorable biophysical properties and potent efficacy. Notably, we have developed a unique and flexible Hybridoma-to-Phage-to-Yeast platform for the generation of CLC bispecific antibodies targeting a given pair of targets.

Keywords: PD-1; PD-L1; common light chain; bispecific antibody; JMB2005

Introduction

Immune checkpoint therapy is considered as a promising strategy for treating cancers. PD-1 is a typical immune checkpoint that limits the response of activated T-cells, and anti-PD-1 monoclonal antibodies (mAbs) have attracted much attention in the field of cancer immunology. Although these antibodies have demonstrated strong potential in cancer treatment during clinical processes, most patients have developed resistance to treatment over time [1]. In addition, monotherapy with antibodies targeting PD-1/PD-L1 has low response rates in most tumor patients, and the benefit remains modest especially in patients with low PD-L1 expression [2]. Therefore, some researchers are inclined to seek for alternative therapeutic strategies for targeting PD-1 with a view to increasing the immune response rate, improving the

efficacy of the immune checkpoint pathway, and demonstrating more promising data in clinical trials [3]. Currently, there are two reported bispecific antibodies (bsAbs) against PD-1 and PD-L1, the LY3434172 and the 609A-based bsAb [4, 5]. LY3434172 is the first antibody against PD-1/PD-L1, and some clinical data on LY3434172 have been released.

BsAb is the most representative component of the new generation of therapeutic strategies, but the implementation of bsAbs and the realization of function are hindered by different challenges, such as expression, stability, and pharmacological properties [6]. The molecular structure of bsAbs is highly complex and diverse; new workflows are needed for molecule expression and cell line development process. Chain mispairing, low expression, and immunogenicity are usually the common challenges,

Received: April 9, 2024. Revised: September 25, 2024. Accepted: October 8, 2024

© The Author(s) 2024. Published by Oxford University Press on behalf of Antibody Therapeutics.

This is an Open Access article distributed under the terms of the Creative Commons Attribution Non-Commercial License (<https://creativecommons.org/licenses/by-nc/4.0/>), which permits non-commercial re-use, distribution, and reproduction in any medium, provided the original work is properly cited. For commercial re-use, please contact journals.permissions@oup.com

resulting in the desired product of interest (POI) being mixed with unwanted product-related impurities that may result in immune responses during the clinical trials [7]. To address these issues, some effective Fab-based engineering strategies have been developed, such as CrossMab [8], common light chain (CLC) [9, 10], orthogonal Fab interface [11], OAscFab-IgG [12], and Wuxibody [13]. Alternatively, Duobody is another method that efficiently generates bsAb molecules through a controlled Fab-arm exchange process [14, 15]. These platforms have been identified as useful strategies that offer great potential for the development of a new generation of bsAbs. Among the many options, CLC appears to be an effective strategy to bypass a number of problems. BsAbs based on CLC do not require additional engineering of the antibody Fc or Fab molecules, such as charge pairing to avoid light chain mispairing, which could have detrimental effects on stability and immunogenicity of the engineered molecules. It is a straightforward solution to avoid light chain mispairings, and it simplifies the purification process in industrial scale manufacture [16, 17].

Compared with traditional mAbs, most bsAbs are more complex in structure and less stable during storage. Therefore, the assessment of the developability should be considered as early as possible during the molecular design and screening processes of bsAbs. The lead molecules with poor developability will have higher failure chances in the later development process [18]. In the developability assessment of mAbs, parameters are assessed based on the differences in physical, chemical, and colloidal stability by techniques such as differential scanning calorimetry (DSC), differential scanning fluorimetry (DSF), and dynamic light scattering (DLS) [19, 20]. In some cases [21, 22], the assessment of developability can be rationally applied to the design and screening of bsAbs. Therefore, it is critical to make full use of the developability assessment strategy in the early stages of bsAbs development to identify cost-effective manufacturable biotherapeutic drugs.

In this study, we reported the discovery and characterization of a potent bsAb, named JMB2005, an IgG-like CLC format that co-targets PD-1 and PD-L1. JMB2005 was generated from the Hybridoma-to-Phage-to-Yeast (H2PtY) platform, which integrated the strength of hybridoma, phage display and yeast display. The platform allowed us to robustly identify (CLC) bsAbs from immunized wild-type mice instead of using engineered CLC transgenic animals that are expensive and are not commonly available in general laboratories. Our data demonstrated that JMB2005 had favorable physicochemical properties and good developability. It exhibits potent activities both *in vitro* and *in vivo*. Specifically, JMB2005 has the potential to be used as a high concentration formulation with great potential benefit in clinical practice.

Materials and methods

Bispecific antibodies identified by the Hybridoma-to-Phage-to-Yeast platform

Firstly, animals were immunized with antigens. Splenocytes were isolated from immunized animals. Anti-PD-1 mAb was obtained through hybridoma technology and antibody engineering technology. To obtain anti-PD-L1 mAb, we screened pre-constructed phage libraries with biotinylated human PD-L1 (Acro, PD1-H82E5). Phage libraries were constructed using V_H genes from PD-L1 immunized animals and the light chain from anti-PD1 mAb. The streptavidin magnetic beads (Thermo Fisher Scientific, Dynabeads M-280) was used to capture the phage binders, which associated with the human biotinylated PD-L1 (Acro, PD1-H82E5).

After two rounds of phage selection, the enriched V_H and the fixed V_K genes were transferred to *Saccharomyces cerevisiae* strain EBY100 (ATCC, MYA-4941) via electroporation, resulting in yeast display Fab library.

Fluorescence activated cell sorting (FACS) was developed to rapidly identify high specific binders for PD-L1. Specifically, the library was incubated with human biotinylated PD-L1, then labeled with mouse anti V5 tag conjugated Alexa Fluor™ 647 (Thermo Fisher, 451098) and streptavidin (SA)-phycoerythrin (PE) (eBioscience, 12-4317-8). The population with double fluorescence positive was sorted by FACSAria II (BD). The collected cells were grown on the plate and picked colony for sequencing and staining evaluation. The colonies with unique sequences were stained with human PD-L1 or irrelevant antigen to confirm the specific PD-L1 binding.

Protein expression and purification.

For transient expression, the candidate sequence containing vectors were transfected into ExpiCHO-S™ cells. After 8–10 days of growth, the supernatant was harvested and purified by AmMag™ Protein A Magnetic Beads (Genscript Biotech, L00695) according to the manufacturer's instruction.

For stable expression, the bsAb sequence containing vectors were transfected into CHO-K1 cells, then antibiotic selection was applied for screening stable cell clones. The obtained clone cells were cultivated for 14 days, harvested and purified by protein A column, buffer exchanged for tests.

Biophysical characterization

Size exclusion chromatography (SEC-HPLC) was carried out to assess the monomer purity of candidates using Waters Alliance e2695 HPLC system with a TOSOH TSK gel G3000WXL column (300 × 7.8 mm, 5 μm). The mobile phase was 200 mM sodium phosphate (pH 6.8), and the flow rate was 0.5 mL/min. Samples were measured by absorbance at a wavelength of 280 nm. Data were analyzed with Waters Empower 3 Enterprise software (Waters, MA, USA).

Hydrophobic interaction chromatography (HIC-HPLC) was performed to evaluate the hydrophobicity of candidates using Waters Alliance e2695 HPLC system with a Thermo MAbPacHIC-10 column (4 × 250 mm, 5 μm). Mobile phase A was 1 M ammonium sulfate with 50 mM sodium phosphate (pH 7.0), and mobile phase B was 50 mM sodium phosphate (pH 7.0). The linear gradient was used, and the flow rate was 0.8 mL/min. Samples were measured at the wavelength of 214 nm. Data were analyzed by Waters Empower 3 Enterprise software (Waters, MA, USA). A shorter retention time indicated that the antibody had increased hydrophilicity.

The pI values and charge variants were characterized by imaged capillary isoelectric focusing (iCIEF) in an iCE3 system (ProteinSimple, CA, USA). Samples were prepared by mixing with pharmalytes, 1% methyl cellulose, pI markers, and water. Samples were pre-focused at 1500 V for 1 min and then focused at 3000 V for 10 min with detection wavelength of 280 nm. Data were acquired by Chrom Perfect software (ProteinSimple, CA, USA) and analyzed by Waters Empower 3 Enterprise software (Waters, MA, USA).

Capillary electrophoresis-sodium dodecyl sulfate (CE-SDS) was performed on a PA800 plus pharmaceutical analysis system purchased from ABScienc (Framingham MA, USA). For non-reducing CE-SDS (nrCE-SDS), samples were diluted and mixed with SDS sample buffer containing IAM, and incubated at 70 °C for 10 min. For reducing CE-SDS (rCE-SDS), β-mercaptoethanol was mixed

with samples and incubated at 70°C for 10 min. Separation was carried out and detected at an absorbance of 220 nm. Data were acquired by 32 Karat software (SCIEX, CA, USA) and then analyzed by Waters Empower 3 Enterprise software (Waters, MA, USA).

The melting temperature (T_m) values of the candidates were measured with a Protein Thermal Shift Dye Kit (Thermo Fisher Scientific, USA). Samples were mixed with Protein Thermal Shift buffer and Protein Thermal Shift dye solution, and then, protein melt curves were assessed in an Applied Biosystems Real-Time PCR System (QuantStudio 3, Thermo Fisher Scientific, USA). Data were analyzed by Protein Thermal Shift Software (version 1.3).

The correctly paired bsAbs were identified and quantified by LC-MS method of intact mass using a Waters Xevo G2-XS Q-TOF (Waters, MA, USA) connected to a Waters ACQUITY UPLC I-ClassBio System, which was equipped with a Waters ACQUITY UPLC BEH300 C4 1.7 μm 2.1 \times 50mm column (Waters, MA, United States). Mobile phase A was 0.1% formic acid (FA) and mobile phase B was 0.1% FA in acetonitrile. Samples were separated using the mobile phase B gradient of 5%–22% in 1 min and then 22%–35% in 11 min. Capillary voltage and source temperature were set at 3.0 kV and 150°C while scanning range was 350–4500 m/z. Data were acquired and analyzed by the Waters UNIFI 1.9.4.053 software (Waters, MA, United States).

Viscosity was evaluated with a viscometer (microVisc TC, RheoSense, San Francisco, CA, USA) coupled to a low viscosity chip (19HA05100415).

Stability evaluation by forced degradation study

To evaluate the stability of candidates and to predict their potential degradation pathways, a series of forced degradation conditions were applied, including 40°C, low pH and high pH. Samples were analyzed by SEC-HPLC to detect aggregates, and iCIEF to measure charge variants and by nrCE-SDS to assess fragments.

To evaluate the stability of JMB2005 at high concentration, short-term stability studies were performed, including 2–8°C, 25°C, and 40°C for up to 4 weeks. Charge variants, aggregates, and fragments of JMB2005 were measured by SE-HPLC, nrCE-SDS, and iCIEF, respectively, for obtaining stability profiling.

Measurement of antibody affinity by bio-layer interferometry

The affinity of bsAbs for human PD-1 (ACRO, PD1-H5221) and PD-L1 (ACRO, PD1-H5229) was measured using Octet Red96 (ForteBio, Sartorius). We used anti-human Fc (AHC) biosensors (ForteBio, 18–5060) to load different BsAbs (5 $\mu\text{g}/\text{mL}$) in kinetics buffer [0.02% Tween-20, 0.1% bovine serum albumin (BSA) in phosphate-buffered saline (PBS)] for 40 s. After immersion for 3 min in kinetics buffer, we incubated the antibody-coated sensors with different concentrations of proteins and recorded association curves for 3 min. Then, we transferred the sensors to wells containing kinetics buffer and recorded dissociation for 10 min. We calculated K_D values with Octet Data Analysis HT 11.0 software using a 1:1 global fit model.

Cell bridging by fluorescence activated cell sorting

PD-1 and PD-L1 expressing CHO-K1 cells were stained with CFSE (Thermo fisher, C34554) and CellTrace Far Red (Thermo Fisher, C34564) following manufacturer's method, respectively. After staining, cells were washed and re-suspended in assay buffer (PBS + 1% BSA). Labeled PD-1 expressing CHO-K1 cells were mixed with the parental anti-PD-1 antibody or isotype control, and labeled PD-L1 expressing CHO-K1 cells were mixed with

titrated JMB2005 or the combination of the parental anti-PD-1 antibody and parental anti-PD-L1 antibody for 2 h at 4°C. The mixture of PD-L1 expressing CHO-K1 cells and antibody was then incubated with the mixture of PD-1 expressing CHO-K1 cells and antibody at a ratio of 1:5, respectively. Samples were analyzed on CytoFLEX flow cytometer (Beckman) after incubating for 48 h at 4°C. FlowJo software was used to gate CFSE+/Far Red-, CFSE-/Far Red+, and CFSE+/Far Red+ events. Percentage of double positive events (CFSE+/Far Red+) was plotted using GraphPad Prism.

Mixed leukocyte reaction

Mature dendritic cells (DCs; PB-DC002F-C) and allogeneic peripheral blood mononuclear cells (PBMCs; PB004F-C) were purchased from OriBiotech. DCs were treated with mitomycin C (Selleckchem, S8146) for 30 min at 37 °C before cocultured with PBMCs at a ratio of 1: 20. Titrated antibodies were added into the coculture system and incubated for 3 d at 37°C. IL-2 secretion in the culture supernatant was measured by enzyme-linked immunosorbent assay (ELISA; R&D Systems, VAL110).

Measurement of binding activity to PD-1 and PD-L1 overexpressing cells by fluorescence activated cell sorting

The cellular binding activity of antibodies to PD-1 and PD-L1 overexpressing cells was evaluated by FACS. Briefly, Jurkat PD-1-NFAT-luc T cells and PD-L1/CHO artificial antigen-presenting cell (aAPC) cells (Promega, J1252) were adjusted at 2×10^6 cells/mL and added 50 μL into U-bottom 96-well plates, respectively. The cells were then incubated with four-fold serially diluted antibodies and incubated for 1 h at 4°C. Subsequently, the cells were washed with washing buffer [PBS + 2% fetal bovine serum (FBS)] and incubated with 250-fold diluted Alexa Fluor™ 488-labeled goat anti-human IgG (H + L) secondary antibody (Invitrogen, A-11013). The samples were analyzed using iQue flow cytometry (Sartorius). Fluorescent signal is plotted as geometric mean fluorescence intensity versus antibody concentration as shown. IC_{50} values were determined with Prism V8.0 software (GraphPad) using a four-parameter logistic curve fitting approach.

Evaluation of PD-1/PD-L1 blockade by reporter gene assay

We conducted the reporter gene assay to evaluate the blockade of PD-1/PD-L1 interaction using a commercially available kit (Promega, J1252). Briefly, PD-L1/CHO (aAPC) cells were seeded at 4×10^4 cells/well in 100 μL in white 96-well plates and cultured overnight at 37°C. The next day, the PD-L1/CHO aAPC cells were incubated with three-fold serially diluted antibodies and Jurkat PD-1-NFAT-luc T cells (5×10^4 /well) that express human PD-1 and luciferases under the control of NFAT response elements in 100 μL RPMI-1640 supplemented with L-glutamine and 1% FBS for 6 h. BioGlo™ Reagent (Promega, G7940) was added to each well and the plates were incubated at room temperature for 10 min. Luminescence was read on an Envision Multimode Plate Reader (PerkinElmer). The luminescent signal was tested as readouts in response to PD-1/PD-L1 pathway blockade.

In vivo efficacy study

NPG mice (5 weeks of age, female) were obtained from Beijing Vitalstar Biotechnology Co., Ltd, and frozen human PBMCs were obtained from Milestone® Biotechnologies. Thawed human

PBMCs and A375 tumor cells (ATCC, Manassas, VA) were co-implanted at a 1:5 E:T ratio into mice to establish the PBMC humanized A375 human melanoma tumor xenograft mouse model for test. After modeling, mice received a dose of 5 mg/kg of test antibodies twice a week via intraperitoneal administration ($n = 8/\text{group}$) for 4 weeks. Human IgG1 was used as isotype control. Pembrolizumab and atezolizumab, as well as their combination, were used as positive controls. Body weight and tumor volumes were measured twice a week starting at 1–2 weeks post-implantation. Tumor volumes were calculated according to the formula ($\text{vol} = 1/2 \times \text{long diameter} \times \text{short diameter}^2$) and plotted as means \pm standard error of the mean (SEM). Data was analyzed using GraphPad Prism (version 8), and statistical analysis of tumor volume data was performed by two-way analysis of variance (ANOVA) followed by Dunnett post-hoc test.

Balb/c-hPD1/hPDL1 Knock-in mice (6–7 weeks of age, female) were obtained from GemPharmatech Co. Ltd. Thawed CT-26-hPDL1 tumor cells (GemPharmatech Co. Ltd) were cultured *in vitro* and implanted into mice on the right hind limb to establish the murine colon cancer mouse model for test. Once the mean tumor volume reached $\sim 80\text{--}100 \text{ mm}^3$, the mice were administered intraperitoneally ($n = 8/\text{group}$) every 3 days with either an isotype control antibody (10 mg/kg), pembrolizumab (5 mg/kg), the parental anti-PD-1 antibody (5 mg/kg), a combination of the parental anti-PD-1 antibody (5 mg/kg) with parental anti-PD-L1 antibody (5 mg/kg), or JMB2005 (5 mg/kg). The study was concluded on the 11th day post-initial drug administration. Tumor volumes were measured and calculated according to the formula ($\text{vol} = 1/2 \times \text{long diameter} \times \text{short diameter}^2$) and plotted as means \pm SEM. Data was analyzed using GraphPad Prism (version 8), and statistical analysis of tumor volume data was performed by two-way ANOVA followed by Dunnett post-hoc test.

In vivo pharmacokinetics study in human FcRn transgenic mouse

A pharmacokinetic study was conducted in human FcRn (hFcRn) transgenic mice. Human FcRn transgenic mice were purchased from Biocytogen (Beijing, CN), 6–8 weeks old male mice were used. Mice received a single dose of 10 mg/kg of test antibody

via intraperitoneal injection ($n = 4/\text{group}$). Serum samples were collected at the following time points: pre-dose, 0.125, 0.292, 1, 2, 3, 4, 7, 10, 14, 21, 28, and 42 days post-dose. Serum concentrations of the antibodies were measured by ELISA. Briefly, anti-human F(ab')_2 (ABCAM, UK) antibody was used as the capture reagent and the mouse anti-human IgG Fc (ABCAM, UK) conjugated to Horseradish Peroxidase (HRP) was used for detection. Data was analyzed using GraphPad Prism (version 8) and pharmacokinetics parameters were determined using Phoenix WinNonlin 8.3 (Certara, NJ, USA).

Results

Generation of humanized common light chain IgG-like bsAb candidates targeting PD-1/PD-L1 based on Hybridoma-to-Phage-to-Yeast platform

The CLC IgG shape bsAb candidates targeting PD-1 and PD-L1 were identified by H2PtY platform. The workflow was shown in Fig. 1. Mice and rats were immunized with antigens PD-1 and PD-L1, respectively. Splenocytes were isolated from immunized animals. Firstly, we obtained murine monoclonal antibodies through hybridoma technology [23] and generated humanized anti-PD-1 mAb by antibody engineering technology [24]. For humanized anti-PD-L1 mAb, heavy chain variable V_H genes were isolated from immunized rats and combined with fixed light chain from the humanized anti-PD-1 mAb to yield a phage display library [25, 26]. The library was screened for 1–2 rounds against PD-L1, and the enriched V_H genes were transferred to yeast surface display [27]. FACS was employed to isolate high affinity V_H genes for PD-L1. PD-L1 specific V_H genes were humanized, and combined with above mentioned humanized anti-PD-1 mAb to assemble into CLC IgG shape bsAbs. IgG1 LALA D265S and knobs-into-hole mutations were introduced into Fc region to avoid the mispairing of two heavy chains. Six bsAb candidates were obtained for further evaluation.

Biophysical characterization of bispecific antibodies candidates

To select a candidate with the lowest risks for manufacture, physicochemical properties of the lead candidates were

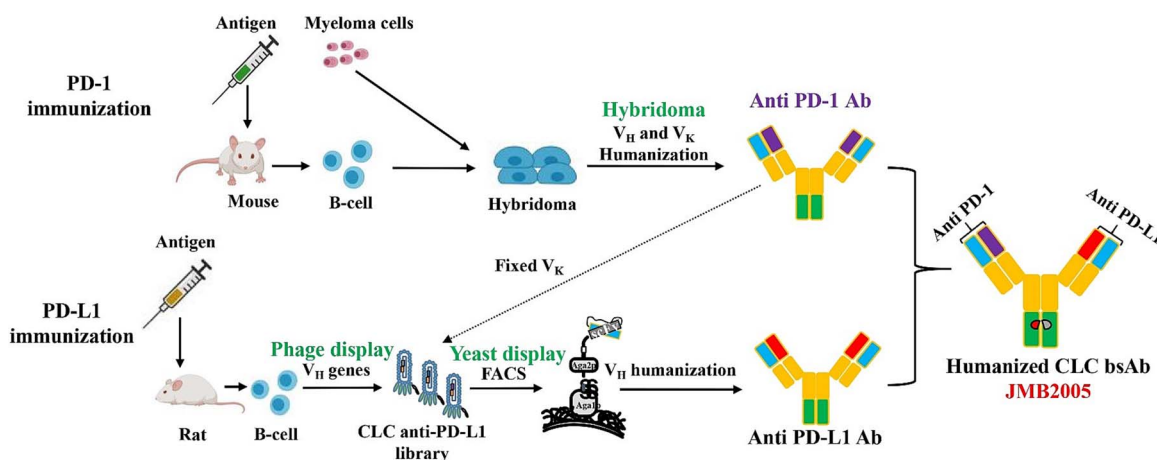


Figure 1. Identification of CLC bsAbs with an H2PtY platform. We first subjected mouse to PD-1 immunization, and subjected rat to PD-L1 immunization. Hybridoma cells were obtained and then antibody engineering and humanization were applied to obtain the humanized anti-PD-1 Ab. In another module, V_H genes from immunized rats were combined with the light chain from the humanized anti-PD-1 mAbs in phage display library, the scFv library was screened, and then transferred to yeast surface. FACS sorting selected V_H genes were humanized and anti-PD-L1 mAbs were identified. Humanized anti-PD-1 and anti-PD-L1 mAbs share the same light chain were assembled to CLC bsAbs candidates, knob-into-hole mutation was inserted into Fc region.

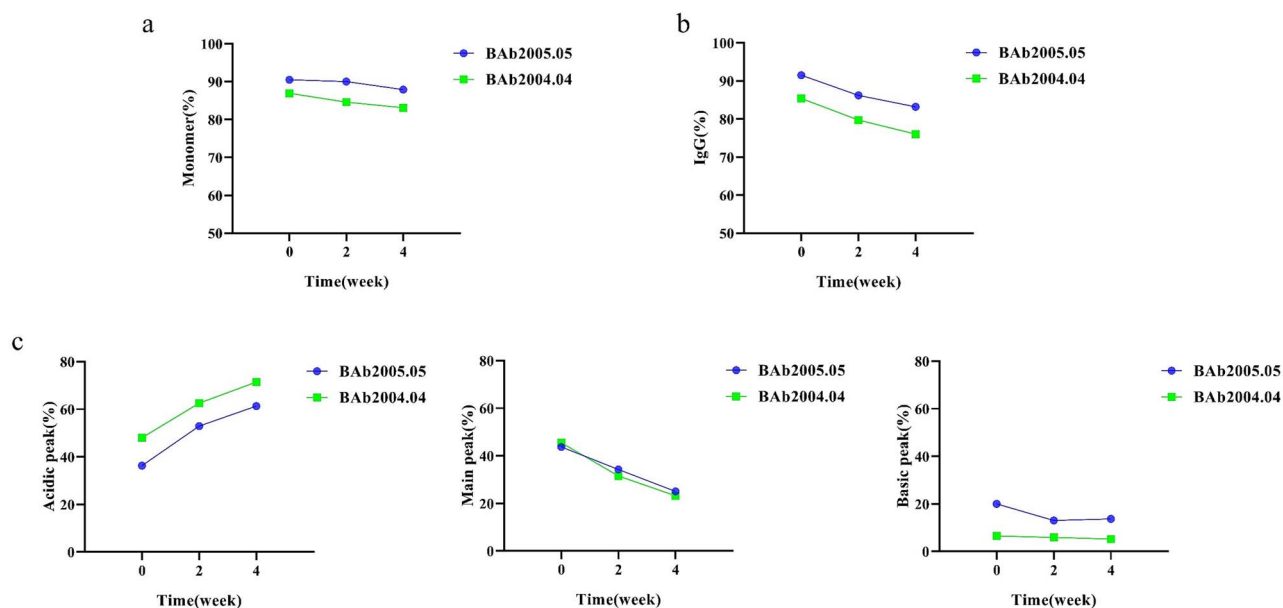


Figure 2. Degradation of bsAb candidates. (a) Change in % monomer measured by SEC-HPLC at 40°C for 4 weeks. (b) Change in %IgG purity measured by nrCE-SDS at 40°C for 4 weeks. (c) Change in % acidic peak, main peak, and basic peak measured by iCIEF at 40°C for 4 weeks.

evaluated. The yield of bsAb candidates was mostly higher than 150 mg/L, except BAb2005.01 and BAb2005.06. Purity was evaluated by SEC-HPLC, nrCE-SDS, and iCIEF. T_m values were evaluated by DSF. Hydrophobicity was evaluated by HIC-HPLC. As showed in Table 1, BAb2005.02 experienced protein precipitation during storage, and BAb2005.03 displayed lower binding affinity to PD-L1. Alternatively, BAb2005.04 and BAb2005.05 exhibited better physicochemical properties, thus were chosen as candidates for further evaluation.

Stability profiling of candidates by forced degradation studies

To predict the stability and to understand in-depth biophysical properties of bsAb candidates, stress condition (40°C) was applied. Samples were taken at different time points and analyzed by SEC-HPLC, nrCE-SDS, and iCIEF. The purity of monomer of both candidates slightly decreased, indicating the lower risk of aggregation for the two candidates (Fig. 2a). The purity decrease of IgG in BAb2005.05 measured by nrCE-SDS was lower than BAb2005.04 (8.3%; and 9.4%, respectively) after 4 weeks at 40°C (Fig. 2b). Major changes in the main peak of two candidates were observed at 40°C, which were primarily due to increased acidic charge variants (Fig. 2c). To sum up, BAb2005.05 showed slower degradation in above mentioned purity profiles, suggesting better stability than BAb2005.04 under the stress condition. Consequently, BAb2005.05 was chosen for further evaluation of functionality, and the molecule was named as JMB2005.

Functionality of JMB2005 *in vitro*

The binding activity of JMB2005 to human PD-1 and PD-L1 was measured by bio-layer interferometry (BLI). JMB2005 bound human PD-1 with a K_D of 0.84 nM, which is 4.5-fold higher than that of pembrolizumab (clinically used anti-PD1 mAb) (Fig. 3a). JMB2005 also bound human PD-L1 with a high affinity ($K_D = 2.33$ nM) but displayed a 6.9-fold lower binding activity than that of atezolizumab (clinically used anti-PD-L1 mAb) (Fig. 3b). Moreover, to determine whether JMB2005 recognized the similar

or different epitope with approved anti-PD-1 pembrolizumab or anti-PD-L1 atezolizumab, an epitope binning experiment using BLI was performed, which demonstrated that JMB2005 showed overlapping binding epitope with pembrolizumab (Supplementary Fig. 2a) and similar epitope with atezolizumab (Supplementary Fig. 2b).

To evaluate whether JMB2005 could engage PD-L1 expressing tumor cells and PD-1 expressing T cells simultaneously, the PD-1 overexpressing (green dye) and PD-L1 overexpressing CHO-K1 (red dye) cells were labeled with fluorescent dyes for *in vitro* test. The FACS pictures with the gating strategy were shown in the Supplementary Fig. 6. Adding JMB2005 into the mixture of PD-1 and PD-L1 expressing CHO-K1 cells resulted in higher percentage of doublets of PD-L1 and PD-1 expressing cells, compared with the combined anti-PD-1 and anti-PD-L1 treated group, the effects of which were abrogated by the addition of anti-PD-1 mAb, confirming the bsAb-mediated engagement of these two cells (Fig. 3c).

To test the specific binding of JMB2005 to PD-1 and PD-L1 expressed on cell surface, PD-1 (Jurkat PD-1-NFAT-luc T cells) and PD-L1 (PD-L1/CHO aAPC cells) overexpressing cells from Promega were used. JMB2005 retained the binding activity to PD-1 and PD-L1 when compared to its parental antibodies. The binding EC_{50} of JMB2005 and its parental anti-PD-1 antibody to Jurkat PD-1-NFAT-luc T cells were 0.77 nM and 0.18 nM (Fig. 3e). The binding EC_{50} of JMB2005 and its parental anti-PD-L1 antibody to PD-L1/CHO aAPC cells were 0.71 nM and 0.15 nM (Fig. 3f). Minimal expression of PD-L1 was also observed on the Jurkat PD-1-NFAT-luc T cells. However, JMB2005 and its parental antibodies had no effect on the luciferase signal when they were incubated with Jurkat PD-1-NFAT-luc T cells without PD-L1/CHO aAPC cells (Supplementary Fig. 3).

To measure the blocking ability of the antibodies on PD-1/PD-L1 interaction, we used a reporter gene assay to test their ability to block PD-1/PD-L1 pathway. PD-L1/CHO aAPC cells were cocultured with Jurkat PD-1-NFAT-luc T cells in the presence of titrated antibodies. Luciferase expression, which was under the control of NFAT response element, was increased in response to

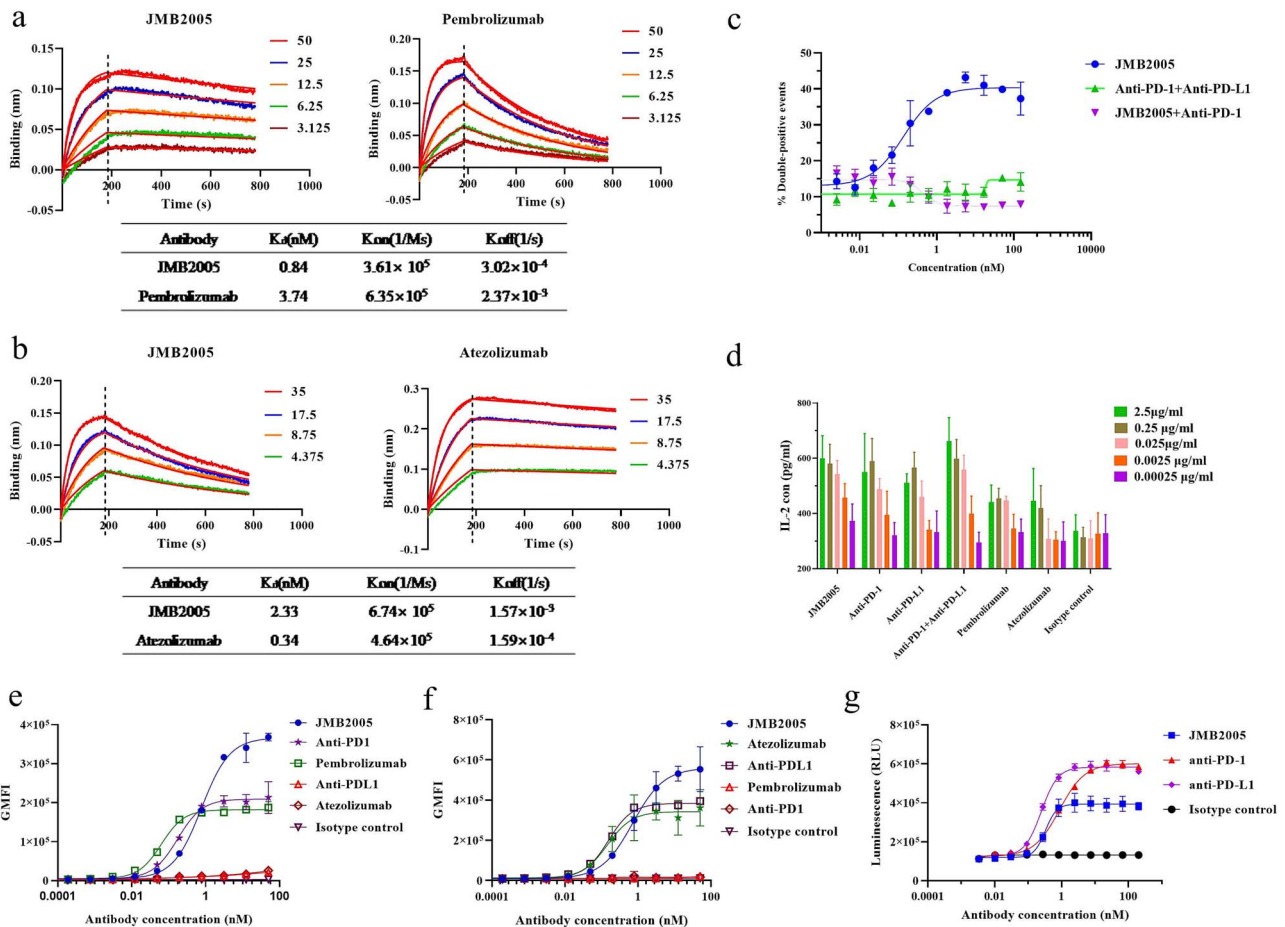


Figure 3. Bioactivity of JMB2005 *in vitro*. (a) Binding affinity to human PD-1 by BLI. (b) Binding affinity to human PD-L1 by BLI. (c) Cell bridging assay by flow cytometry. (d) MLR of allogeneic immature DCs and CD4 T cells in the presence of test antibodies as indicated. IL-2 level in the culture media was determined by ELISA. (e) Binding activity to Jurkat PD-1-NFAT-luc T cells. (f) Binding activity to PD-L1/CHO aAPC cells. (g) Inhibition of PD-1/PD-L1 pathway.

JMB2005, anti-PD-1 or anti-PD-L1 treatment, with EC_{50} values of 0.33, 0.86, and 0.25 nM, respectively (Fig. 3g). Moreover, JMB2005 also blocked the binding of human PD-L2 to PD-1 overexpressing cells ($IC_{50} = 0.83 \mu\text{g/ml}$; Supplementary Fig. 4).

To test the ability of JMB2005 in promoting T cell responses, mixed leukocyte reaction (MLR) assay was applied by coculturing mature DCs and allogeneic PBMCs, and the secretion of IL-2 was measured as a hallmark for T cell activation. The blockade of PD-1/PD-L1 pathway by JMB2005 displayed a titratable enhancement of IL-2 release with comparable efficacy to the combination of anti-PD-1 and anti-PD-L1 group (Fig. 3d). Meanwhile, the functional activity of JMB2005 was higher than that of the pembrolizumab or atezolizumab monotreatment. In short, JMB2005 can promote T cell activation *in vitro* and shows better efficacy than pembrolizumab or atezolizumab monotreatment.

Therapeutic efficacy of JMB2005 *in vivo*

To verify the *in vivo* antitumor efficacy, JMB2005 was evaluated in the humanized A375 human melanoma tumor xenograft mouse models that co-implanted with human PBMCs, and was compared with pembrolizumab [28, 29], atezolizumab [30, 31], and their combination, respectively. As shown in Fig. 4a, JMB2005 treatment resulted in significant tumor growth inhibition (TGI) and prominent complete responses (CRs) at the dose of 5 mg/kg (100%TGI; 8/8 CRs). The antitumor activity of JMB2005 was superior to that

of pembrolizumab, atezolizumab monotreatment, and their combination treatment (22.5%TGI, 0/8 CRs; 82.3%TGI, 1/8 CRs; and 58.9%TGI, 0/8 CRs, respectively). In addition, no obvious toxicity was observed in animals of JMB2005 treatment, as revealed by body weight measurement. These results collectively confirmed that JMB2005 was effective and safe.

Encouraging results were also observed in the genetically engineered Balb/c-hPD1/hPDL1 knock-in mouse model bearing with CT-26-hPDL1 tumors. The genetically engineered Balb/c-hPD1/hPDL1 knock-in mice have intact immune system, with normal development of macrophages and T cells, potentially reflecting the impact of T-macrophage interaction on antitumor responses. We compared the anti-tumor efficacy of JMB2005 with its parental mAbs targeting PD-1 or PD-L1 in this model. As shown in Fig. 4b, the antitumor activity of JMB2005 was superior to that of pembrolizumab treatment, the parental anti-PD-1 monotherapy, or the combined therapy of the parental anti-PD-1 with parental anti-PD-L1 (74.58% TGI, 40.07% TGI, 67.28% TGI, and 67.63% TGI, respectively).

Collectively, the results of *in vivo* efficacy suggested that JMB2005 as a bsAb was more efficient than the anti-PD-1 or anti-PD-L1 monotreatment as well as the anti-PD-1 and anti-PD-L1 combination treatment. The blockade of both PD-1 and PD-L1, and the induction of cell-to-cell bridging by JMB2005, together contributed to the enhancement of T-cell activation and antitumor immune responses.

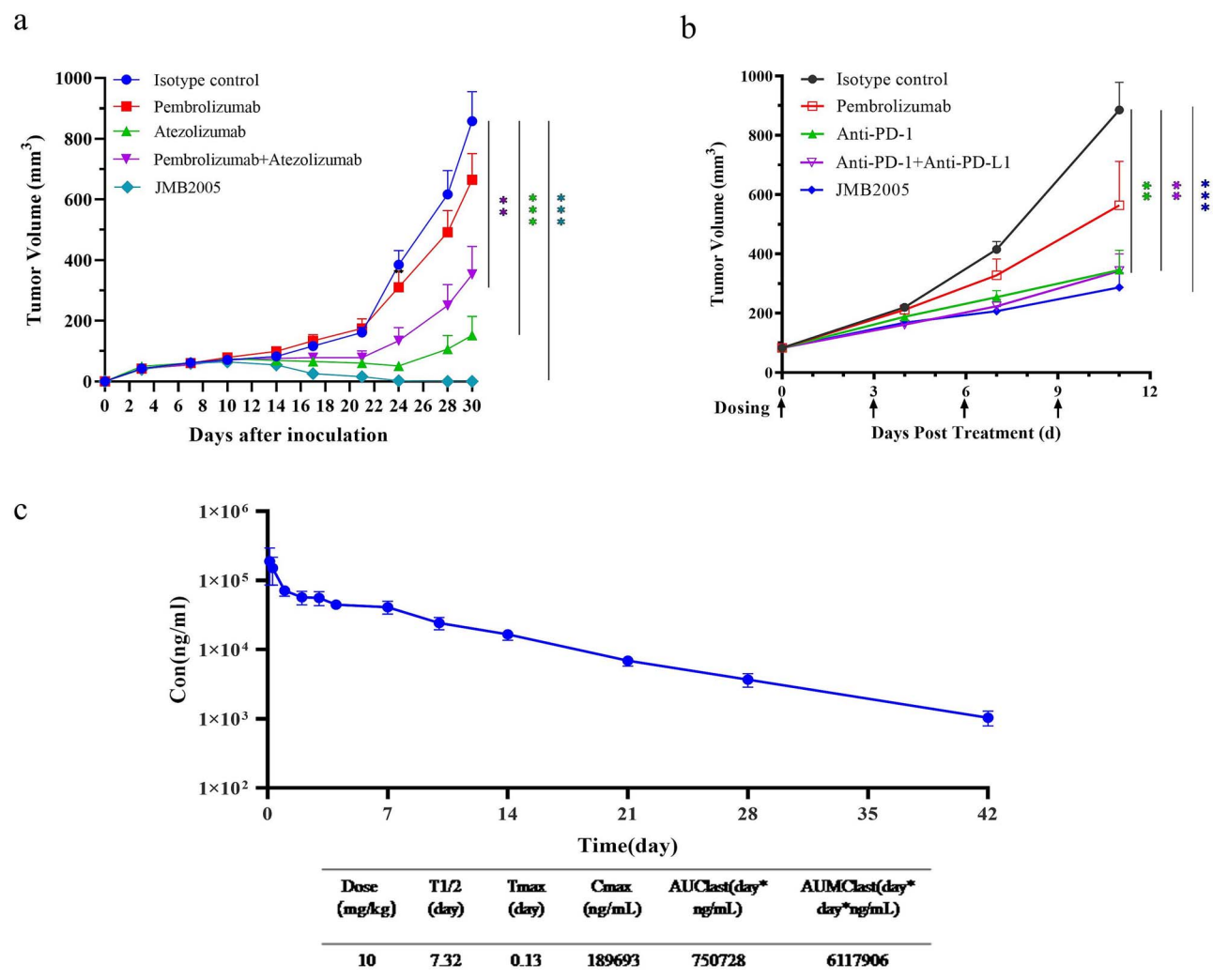


Figure 4. Antitumor efficacy and PK study of JMB2005 *in vivo*. (a) In A375 human tumor xenograft mouse model, 40 tumor-bearing mice were divided into 5 groups. Statistically significant tumor volume reduction by JMB2005 at a dose of 5 mg/kg compared to the isotype control group. (b) In CT-26-hPDL1 murine colon cancer model, 40 Balb/c-hPD1/hPDL1 knock-in mice-bearing CT-26-hPDL1 tumors were divided into 5 groups and subjected to their respective treatment regimens. JMB2005, administered at a dosage of 5 mg/kg, demonstrated a statistically significant reduction in tumor volume relative to the isotype control group. (* $P < 0.05$, ** $P < 0.01$, *** $P < 0.001$, **** $P < 0.0001$ vs isotype control group). (c) Pharmacokinetics detection of JMB2005 in hFcRn transgenic mice.

Pharmacokinetics of JMB2005 in hFcRn transgenic mice

To evaluate the serum PK profile, JMB2005 was administrated to hFcRn transgenic mice at a single intraperitoneal dose of 10 mg/kg. Serum samples were collected and analyzed by ELISA assay. As indicated in Fig. 4c, JMB2005 exhibited a typical human IgG PK profile with a half-life ($T_{1/2}$) of 7.32 days.

Manufacturability evaluation of JMB2005

JMB2005, a potent anti-PD1/PD-L1 bsAb, demonstrated desired biophysical properties, good stability, and pharmacokinetics *in vivo*, and enhanced efficacy *in vitro* and *in vivo*. Based on these excellent characteristics, JMB2005 was pushed into the CMC development stage to evaluate its manufacturability.

For the bsAbs production, the JMB2005 transfectant CHO cells were cultivated for 14 days, then harvested, and bsAb was purified by protein A column. The expression titer of JMB2005 was ~5 g/L. With one-step protein A affinity chromatography purification, the purity of JMB2005 reached 90.3%, 92.3%, and 98.6%, respectively, as measured by SEC-HPLC, nrCE-SDS, and rCE-SDS (Table 2). The

charge variants were <28% as measured by iCIEF, the percentage of correctly paired bsAb was up to 88.9%, as monitored by LC-MS method (Table 2). Importantly, JMB2005 can be purified by adopting the existing IgG monoclonal antibody purification process, and the correctly pair rate of the bsAb increased to >95% after further purification, suggesting the good manufacturability of JMB2005.

Evaluation of developability of high concentration preparations

There is a growing demand for subcutaneous delivery of biologics due to the great convenience in clinical use, both for physicians and patients [19]. Limited protein solubility is a major challenge for the subcutaneous route of administration [32], and stability and viscosity are often key factors determining the development of highly concentrated formulations [33]. Solubility and associated viscosity are evaluated to verify whether JMB2005 has the potential to be concentrated at a high concentration for subcutaneous injection. As shown in Fig. 5d, JMB2005 had a viscosity of <6 mpa at the concentration of 120 mg/mL, indicating good solubility

Table 1. Physicochemical properties of bsAb candidates.

Antibody	Purity by SEC-HPLC (monomer %)	Fab T _m (°C)	Hydrophobicity (min)	pI value	Charge variants by iCIEF		Purity by CE-SDS (IgG %)	Precipitation	Binding affinity to PDL1 (nM)
					Acidic peaks (%)	Main peak (%)			
BAb2005.01	88.95	82.20	14.5	9.1	31.7	51.8	89.8	/	/
BAb2005.02	90.68	82.95	13.9	9.0	30.2	50.2	90.1	Yes	/
BAb2005.03	92.16	82.95	13.9	9.1	26.5	51.9	90.8	No	0.1276
BAb2005.04	92.94	82.95	13.9	9.0	24.2	53.5	93.0	No	0.04107
BAb2005.05	92.09	81.91	14.3	9.1	28.2	54.5	94.4	No	0.05612
BAb2005.06	87.66	83.69	14.0	9.3	22.9	55.7	95.8	/	/

and low viscosity of JMB2005 allowed the potential development into high concentration solution for subcutaneous injection. High temperature stress conditions can offer an opportunity to understand major degradation pathway of candidates and provide a foundation for further formulation development [34]. To gain a first understanding about how JMB2005 at high concentration will degrade, short-term stability studies were performed. JMB2005 was concentrated to 120 mg/mL in 20 mM histidine buffer at pH 5.5 and staged at 5°C, 25°C, and 40°C for up to 4 weeks. As shown in Fig. 5a–c, no obvious changes were observed in the purity of monomer, IgG, and charge variants at 5°C for 4 weeks, indicating the good stability of JMB2005 at a high concentration of 120 mg/mL at 5°C. No decrease of monomer and IgG was observed, and little reduction in the purity of main peak was found at 25°C for 4 weeks, suggesting the good stability of JMB2005 at high concentration at room temperature. Decrease in purity was observed at 40°C, the main degradation products were fragments (Supplementary Fig. 1b) and acidic variants (Fig. 5c). No significant aggregation was induced under high temperature conditions (Supplementary Fig. 1a), suggesting the lower risk of aggregation tendency. At this stage of development, the formulation had not been optimized. Excipients can provide stabilizing effects and reduce protein degradation [35, 36]. There is room to optimize the formulation and improve the stability of JMB2005 at high protein concentration in the future. Together, our results show that JMB2005 has the potential to be formulated at a high concentration as an effective subcutaneous injectable bsAb for clinical usage.

Discussion

Immune checkpoint blockade strategies targeting “PD-1/PD-L1” have displayed superior anti-tumor efficacy against many cancers in the clinical practice [37]. However, <30% of patients maintain a sustained clinical response during anti-PD-1 or anti-PD-L1 monotherapy, and a large percentage of patients do not benefit from the therapy, or develop more complex conditions in advanced stages [38]. Follow-up cases demonstrate that simultaneous blockage of PD-1 and PD-L1 can further inhibit the PD-1 pathway and promote bridging between PD-1 expressing T cells and PD-L1-positive tumor cells in tumor microenvironment, suggesting that co-targeting PD-1 and PD-L1 with bsAbs might be an effective way to improve clinical efficacy. In this study, we described the discovery of a CLC bsAb, and the preclinical studies verified the hypothesis that simultaneously blocking both PD-1 and PD-L1 pathways can increase the immune response and improve the antitumor efficacy. BsAbs co-targeting PD-1 and PD-L1 may have greater potential to improve the efficacy of the immune checkpoint pathway.

The concept of using a CLC format to efficiently produce a whole IgG shape bsAb was firstly reported by Merchant et al. in 1998, and the proposed notion of heterodimerization of the Fc region by means of “knobs-into-holes” provided a new strategy for the development of bsAbs. In the industrial manufacture of bsAbs, the “CLC format” is an effective technique that reduces mispairing between heavy and light chains and avoids related manufacturability issues. Furthermore, it is possible to maintain the natural molecular state of the antibody while introduce bispecific functionality. CLC bsAbs have been developed by a variety of different strategies. For example, McWhirter et al. created transgenic mice with a fixed CLC and successfully identified a human bsAb with CLC from the mice (WO2011097603). Smith et al. described the VelocImmune[®] mouse anti-CD-20/CD-3 CLC

Table 2. Physicochemical properties of JMB2005 after one-step protein A purification from stable cell line in the CMC stage.

Antibody	Purity by SEC-HPLC (monomer %)	Charge variants by iCIEF			Purity by nrCE-SDS (IgG %)	Purity by rCE-SDS (LC + HC %)	Correctly paired bsAb (%)
		Acidic peaks (%)	Main peak (%)	Basic peaks (%)			
JMB2005	90.3	21.0	72.4	6.6	92.3	98.6	88.9

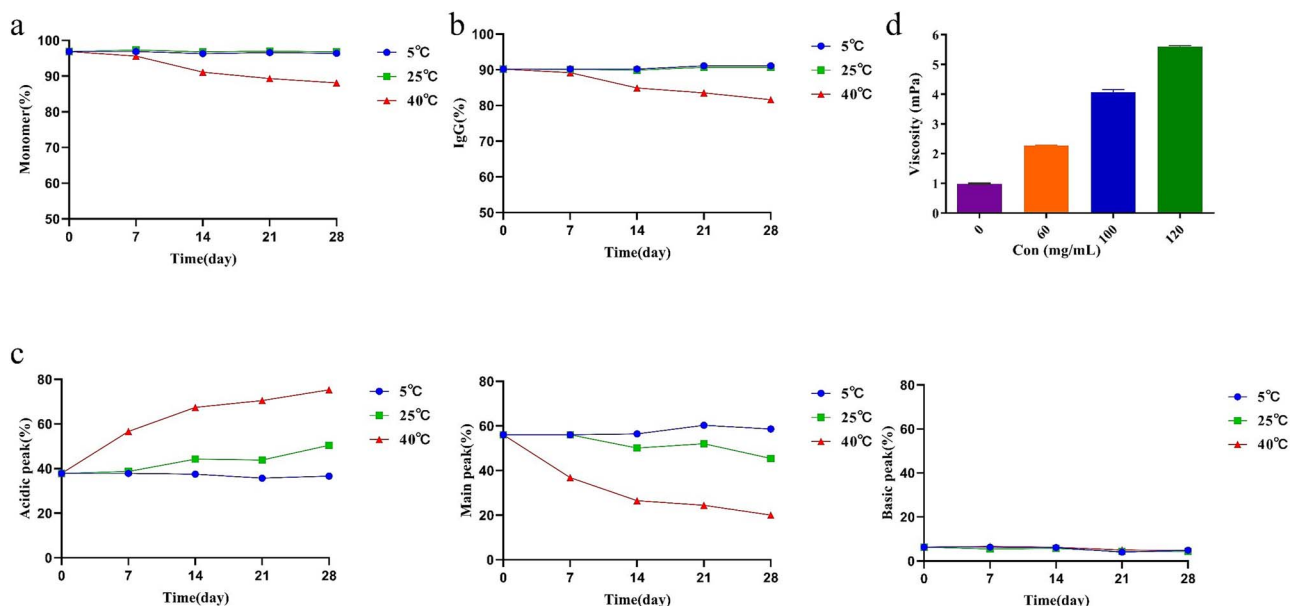


Figure 5. Stability evaluation of JMB2005 at 120 mg/mL. (a) Change in % monomer measured by SEC-HPLC at 5°C, 25°C and 40°C for 28 days. (b) Change in %IgG measured by CE-SDS at 5°C, 25°C and 40°C for 28 days. (c) Change in % acidic peak, main peak and basic peak measured by iCIEF at 5°C, 25°C and 40°C for 28 days. (d) Viscosity measurement at 0 mg/mL, 60 mg/mL, 100 mg/mL and 120 mg/mL.

bsAb [39]. Krah et al. successfully obtained bsAbs with a CLC combined with animal immunization and yeast display [16]. Based on previous experience [40], bsAbs identified by screening naive CLC antibody libraries have low affinity and low successful rates. Here, we report H2PtY platform for the efficient discovery of CLC bsAbs with good affinity and developabilities. H2PtY is an upgraded version of the PtY platform [41, 42], where we have added animal immunization and hybridoma technology to our existing PtY platform [23]. By the combination of hybridoma and PtY, the success rate of the discovery of CLC bsAbs was significantly improved. The low affinity issue is also largely solved. By immunizing the animals, we obtained a murine antibody against PD-1 and used its humanized light chain sequence to recombine with the antibody heavy chain variable region (V_H) sequences of human PD-L1-immunized rat spleen cells, to construct a CLC single chain (scFv) phage antibody library [25, 26]. After phage screening, the PD-L1 scFv antibody sequences were transferred to yeast display and were screened by FACS [27]. Anti-PD-L1 murine V_H sequences were selected and humanized [24]. The humanized anti-PD-1 heavy chain, anti-PD-L1 heavy chain, and their CLC were assembled into a bsAb. The H2PtY platform has the following unique features: (i) traditional wild-type mice was allowed to be used to provide antibody genes to CLC bsAb discovery in general laboratories. (ii) For any given pair of targets, the success rate of bsAb discovery was almost 100% in our lab, which is in good alignment with a recent report that functional antibodies from immunized animals exhibit light chain coherence [40]. (iii) The bsAb molecules discovered by H2PtY platform have reasonably high affinity toward both arms, normally $\sim 10^{-9}$ M (Supplementary

Table 1). Admittedly, the platform also has its disadvantages, e.g.: we need to individually immunize the animals with individual antigens. Efforts are needed to generate hybridoma mAb for one of the antigens, which may increase the screening efforts. Interestingly, we have noticed that when one of the two antigens has a lower immune response, we need to generate a candidate mAb for this lower immune response antigen by hybridoma technology, and the humanized light chain of this mAb should be used in the H2PtY platform to improve the success rate of CLC bsAb discovery.

Based on the available data, JMB2005 was deemed to comply with CMC operations, and has favorable developability. It showed high titer, and one-step protein A purification yielded high rate of correctly paired bsAb products. In addition, JMB2005 exhibited good solubility, lower viscosity, low risk of aggregation tendency, and good short-term stability at high concentration under lower temperature, suggesting the potential of subcutaneous administration for clinical applications.

Targeting simultaneously to PD-1 and PD-L1, JMB2005 can bridge tumor cells and T-cells, and can promote T-cells to play a direct role in killing tumor cells. In previous studies, bsAbs of anti-PD-1/PD-L1 were also able to block PD-L1 on DCs from binding to CD80, bridging DC cells and T cells and promoting T cell activation. This mechanism of action is not shared by PD-1 monoclonal antibody, PD-L1 monoclonal antibody, or the combination of both. Therefore, JMB2005 has better cell-bridge function and lymphocyte activation function, which is superior to a mAb monotreatment. Furthermore, in both tumor models, JMB2005 showed better *in vivo* tumor suppression activity

compared to anti-PD-1 and anti-PD-L1 monotherapy as well as the combination of both.

In terms of the mechanisms of action, JMB2005 showed dual-target desired efficacy in pre-clinical studies. It bound to both PD-1 and PD-L1 monovalently or simultaneously, and effectively block the PD-1/PD-L1 pathway. However, the tumor microenvironment in patients was relatively complex. Not all cancers respond to checkpoint inhibitors and many tumors progress following initial treatment, suggesting that additional immunosuppressive factors, such as regulatory T cells, might be present that inhibit anti-tumor responses. PDL1 is also expressed on activated T cells. As previous studies identified [43, 44], PD-L1 ligation on human CD25-depleted CD4+ T cells, combined with CD3/TCR stimulation, induces their conversion into highly suppressive T cells. We also found that JMB2005 induced the conversion of memory T cells to inducible regulatory T cells (iTregs) in the combination of CD3/TCR stimulation (Supplementary Fig. 5). The results could have important consequences for the ability of the immune system to respond to infections and affect the efficacy of immune checkpoint immunotherapy against cancer. To illustrate, some studies as reported [45–47] had shown that PD-1/PD-L1 inhibitors combined with Treg-modulating agents were expected to enhance the sensitivity of patients to anti-PD-1/PD-L1 therapy. These findings provide a basis for further investigation in the future.

Moreover, a new study has also found that PD-L1 expressed T cells interacted with PD-1 expressed macrophage, leading to macrophage suppression [48]. Although JMB2005 exerts either PD1/PDL1 blockade effect or a bridging effect for dual blockage, we do not exclude the possibilities of a suppressive effect of JMB2005 on macrophage phenotype. Considering the complex nature of PD1/PDL1 axis blockade which complicated involved in dose, affinity, and PD-1 target saturation in the tumor. We will keep exploring this potential mechanism of macrophage suppression. Collectively, whether the unique mechanism of action of JMB2005 can be translated into clinical practice and exert the expected effects requires more exploration in the future, including clinical safety and efficacy validation.

In conclusion, we reported the successful discovery and development process of anti-PD1/PD-L1 CLC bsAb JMB2005 in the present study. JMB2005 showed enhanced T-cell activation property *in vitro*, outstanding anti-tumor efficacy and favorable half-life *in vivo*. Furthermore, JMB2005 demonstrated excellent biophysical properties, good stability, desired manufacturing characteristics as IgG shape antibodies, and high potential of subcutaneous injection for clinical usage. Therefore, JMB2005 has the potential to achieve good clinical outcomes, providing a new promising immunotherapy for cancer treatment in the future. Notably, we reported a promising unique and flexible CLC bsAbs discovery platform, which could be applied to identify more potential CLC bsAbs targeting different targets for clinical usage.

Acknowledgements

The authors thank Haifeng Cui, Xun Fan, Xueping Wang, and Ling Cai from Shanghai Jemincare Pharmaceutical Co., Ltd. for supporting the program.

Author contributions

Sujun Deng (Directed the project and reviewed the manuscript), Haixiang Yu (Provided technical guidance and reviewed the manuscript), Peipei Liu (Led the project, designed developability experiments and wrote the manuscript), Chunyin Gu and Zongda

Wang (Designed and performed antibodies discovery), Huawei Zhang and Yukun Yang (Performed biophysical analysis), Xiaodan Cao (Designed *in vitro* experiments), Fangfang Jia and Xianqing He (Performed *in vitro* experiments), Kedong OuYang and Yingying Zhen (Designed *in vivo* animal experiments).

Supplementary data

Supplementary data is available at ABT online.

Conflict of interest

Peipei Liu, Chunyin Gu, Xiaodan Cao, Huawei Zhang, Zongda Wang, Yukun Yang, KeDong OuYang, Yingying Zhen, Fangfang Jia, Xianqing He, Haixiang Yu, and Sujun Deng are employees of Shanghai Jemincare Pharmaceutical Co., Ltd.

Funding

This research was funded and supported by Shanghai Jemincare Pharmaceutical Co., Ltd.

Data availability

The data will be available from the corresponding author upon reasonable request.

Ethics and consent statement

Not applicable.

Animal research statement

The *in vivo* antitumor efficacy study protocol was approved by Institutional Animal Care and Use Committee (IACUC) of PharmaLegacy Laboratories (Shanghai) Co., Ltd or by the IACUC of GemPharmatech Co., Ltd. Other animal study protocols were approved by the IACUC of Charles River Medical Technology (Shanghai) Co., Ltd.

References

1. Akinleye A, Rasool Z. Immune checkpoint inhibitors of PD-L1 as cancer therapeutics *J Hematol Oncol*. 2019;**12**:92. <https://doi.org/10.1186/s13045-019-0779-5>.
2. Gong J, Chehrizi-Raffle A, Reddi S. et al. Development of PD-1 and PD-L1 inhibitors as a form of cancer immunotherapy: a comprehensive review of registration trials and future considerations *J Immunother Cancer*. 2018;**6**:8. <https://doi.org/10.1186/s40425-018-0316-z>.
3. Topalian SL, Hodi FS, Brahmer JR. et al. Five-year survival and correlates among patients with advanced melanoma, renal cell carcinoma, or non-small cell lung cancer treated with nivolumab *JAMA Oncol*. 2019;**5**:1411–20. <https://doi.org/10.1001/jamaoncol.2019.2187>.
4. Kotanides H, Li Y, Malabunga M. et al. Bispecific targeting of PD-1 and PD-L1 enhances T-cell activation and antitumor immunity *Cancer Immunol Res*. 2020;**8**:1300–10. <https://doi.org/10.1158/2326-6066.CIR-20-0304>.
5. Zhao J, Jiang L, Yang H. et al. A strategy for the efficient construction of anti-PD1-based bispecific antibodies with desired IgG-like properties *MAbs*. 2022;**14**:2044435. <https://doi.org/10.1080/19420862.2022.2044435>.

6. Shim H. Bispecific antibodies and antibody-drug conjugates for cancer therapy: technological considerations *Biomolecules*. 2020;**10**:360. <https://doi.org/10.3390/biom10030360>.
7. Tevelev B, Patel H, Shields K. et al. Genetic rearrangement during site specific integration event facilitates cell line development of a bispecific molecule *Biotechnol Prog*. 2021;**37**:e3158. <https://doi.org/10.1002/btpr.3158>.
8. Klein C, Schaefer W, Regula JT. et al. Engineering therapeutic bispecific antibodies using CrossMab technology *Methods*. 2019;**154**:21–31. <https://doi.org/10.1016/j.ymeth.2018.11.008>.
9. Van Blarcom T, Lindquist K, Melton Z. et al. Productive common light chain libraries yield diverse panels of high affinity bispecific antibodies *MAbs*. 2018;**10**:256–68. <https://doi.org/10.1080/19420862.2017.1406570>.
10. Merchant AM, Zhu Z, Yuan JQ. et al. An efficient route to human bispecific IgG *Nat Biotechnol*. 1998;**16**:677–81. <https://doi.org/10.1038/nbt0798-677>.
11. Wu X, Yuan R, Bacica M. et al. Generation of orthogonal fab-based trispecific antibody formats *Protein Eng Des Sel*. 2018;**31**:249–56. <https://doi.org/10.1093/protein/gzy007>.
12. Schanzer JM, Wartha K, Croasdale R. et al. A novel glyco-engineered bispecific antibody format for targeted inhibition of epidermal growth factor receptor (EGFR) and insulin-like growth factor receptor type I (IGF-1R) demonstrating unique molecular properties *J Biol Chem*. 2014;**289**:18693–706. <https://doi.org/10.1074/jbc.M113.528109>.
13. Guo G, Han J, Wang Y. et al. A potential downstream platform approach for WuXiBody-based IgG-like bispecific antibodies *Protein Expr Purif*. 2020;**173**:105647. <https://doi.org/10.1016/j.pep.2020.105647>.
14. Labrijn AF, Meesters JI, de Goeij BE. et al. Efficient generation of stable bispecific IgG1 by controlled fab-arm exchange *Proc Natl Acad Sci U S A*. 2013;**110**:5145–50. <https://doi.org/10.1073/pnas.1220145110>.
15. Labrijn AF, Meesters JI, Priem P. et al. Controlled fab-arm exchange for the generation of stable bispecific IgG1 *Nat Protoc*. 2014;**9**:2450–63. <https://doi.org/10.1038/nprot.2014.169>.
16. Krah S, Schröter C, Eller C. et al. Generation of human bispecific common light chain antibodies by combining animal immunization and yeast display *Protein Eng Des Sel*. 2017;**30**:291–301. <https://doi.org/10.1093/protein/gzw077>.
17. Shiraiwa H, Narita A, Kamata-Sakurai M. et al. Engineering a bispecific antibody with a common light chain: identification and optimization of an anti-CD3 epsilon and anti-GPC3 bispecific antibody, ERY974 *Methods*. 2019;**154**:10–20. <https://doi.org/10.1016/j.ymeth.2018.10.005>.
18. Zhang W, Wang H, Feng N. et al. Developability assessment at early-stage discovery to enable development of antibody-derived therapeutics *Antib Ther*. 2022;**6**:13–29. <https://doi.org/10.1093/abt/tbac029>.
19. Zarzar J, Khan T, Bhagawati M. et al. High concentration formulation developability approaches and considerations *MAbs*. 2023;**15**:2211185. <https://doi.org/10.1080/19420862.2023.2211185>.
20. Yang X, Xu W, Dukleska S. et al. Developability studies before initiation of process development: improving manufacturability of monoclonal antibodies *MAbs*. 2013;**5**:787–94. <https://doi.org/10.4161/mabs.25269>.
21. Jarasch A, Koll H, Regula JT. et al. Developability assessment during the selection of novel therapeutic antibodies *J Pharm Sci*. 2015;**104**:1885–98. <https://doi.org/10.1002/jps.24430>.
22. Müller T, Tasser C, Tesar M. et al. Selection of bispecific antibodies with optimal developability using FcRn-Ph-HPLC as an optimized FcRn affinity chromatography method *MAbs*. 2023;**15**:2245519. <https://doi.org/10.1080/19420862.2023.2245519>.
23. Köhler G, Milstein C. Continuous cultures of fused cells secreting antibody of predefined specificity *Nature*. 1975;**256**:495–7. <https://doi.org/10.1038/256495a0>.
24. Jones PT, Dear PH, Foote J. et al. Replacing the complementarity-determining regions in a human antibody with those from a mouse *Nature*. 1986;**321**:522–5. <https://doi.org/10.1038/321522a0>.
25. Smith GP. Filamentous fusion phage: novel expression vectors that display cloned antigens on the virion surface *Science*. 1985;**228**:1315–7. <https://doi.org/10.1126/science.4001944>.
26. McCafferty J, Griffiths AD, Winter G. et al. Phage antibodies: filamentous phage displaying antibody variable domains *Nature*. 1990;**348**:552–4. <https://doi.org/10.1038/348552a0>.
27. Boder ET, Wittrup KD. Yeast surface display for screening combinatorial polypeptide libraries *Nat Biotechnol*. 1997;**15**:553–7. <https://doi.org/10.1038/nbt0697-553>.
28. Kwok G, Yau TC, Chiu JW. et al. Pembrolizumab (Keytruda) *Hum Vaccin Immunother*. 2016;**12**:2777–89. <https://doi.org/10.1080/21645515.2016.1199310>.
29. Longoria TC, Tewari KS. Evaluation of the pharmacokinetics and metabolism of pembrolizumab in the treatment of melanoma *Expert Opin Drug Metab Toxicol*. 2016;**12**:1247–53. <https://doi.org/10.1080/17425255.2016.1216976>.
30. Li M, Zhao R, Chen J. et al. Next generation of anti-PD-L1 atezolizumab with enhanced anti-tumor efficacy in vivo *Sci Rep*. 2021;**11**:5774. <https://doi.org/10.1038/s41598-021-85329-9>.
31. Herbst RS, Giaccone G, de Marinis F. et al. Atezolizumab for first-line treatment of PD-L1-selected patients with NSCLC *N Engl J Med*. 2020;**383**:1328–39. <https://doi.org/10.1056/NEJMoa1917346>.
32. Shire SJ, Shahrokh Z, Liu J. Challenges in the development of high protein concentration formulations *J Pharm Sci*. 2004;**93**:1390–402. <https://doi.org/10.1002/jps.20079>.
33. Wang SS, Yan YS, Ho K. US FDA-approved therapeutic antibodies with high-concentration formulation: summaries and perspectives *Antib Ther*. 2021;**4**:262–72. <https://doi.org/10.1093/abt/tbab027>.
34. Xu Y, Wang D, Mason B. et al. Structure, heterogeneity and developability assessment of therapeutic antibodies *MAbs*. 2019;**11**:239–64. <https://doi.org/10.1080/19420862.2018.1553476>.
35. Strickley RG, Lambert WJ. A review of formulations of commercially available antibodies *J Pharm Sci*. 2021;**110**:2590–2608.e56. <https://doi.org/10.1016/j.xphs.2021.03.017>.
36. Ghosh I, Gutka H, Krause ME. et al. A systematic review of commercial high concentration antibody drug products approved in the US: formulation composition, dosage form design and primary packaging considerations *MAbs*. 2023;**15**:2205540. <https://doi.org/10.1080/19420862.2023.2205540>.
37. Yi M, Zheng X, Niu M. et al. Combination strategies with PD-1/PD-L1 blockade: current advances and future directions *Mol Cancer*. 2022;**21**:28. <https://doi.org/10.1186/s12943-021-01489-2>.
38. Wang Q, Wu X. Primary and acquired resistance to PD-1/PD-L1 blockade in cancer treatment *Int Immunopharmacol*. 2017;**46**:210–9. <https://doi.org/10.1016/j.intimp.2017.03.015>.
39. Smith EJ, Olson K, Haber LJ. et al. A novel, native-format bispecific antibody triggering T-cell killing of B-cells is robustly active in mouse tumor models and cynomolgus monkeys *Sci Rep*. 2015;**5**:17943. <https://doi.org/10.1038/srep17943>.
40. Jaffe DB, Shahi P, Adams BA. et al. Functional antibodies exhibit light chain coherence *Nature*. 2022;**611**:352–7. <https://doi.org/10.1038/s41586-022-05371-z>.

41. Gu C, Cao X, Wang Z. et al. A human antibody of potent efficacy against SARS-CoV-2 in rhesus macaques showed strong blocking activity to B.1.351 MAbs. 2021;**13**:1930636. <https://doi.org/10.1080/19420862.2021.1930636>.
42. Yin W, Xu Y, Xu P. et al. Structures of the omicron spike trimer with ACE2 and an anti-omicron antibody *Science*. 2022;**375**: 1048–53. <https://doi.org/10.1126/science.abn8863>.
43. Fanelli G, Romano M, Nova-Lamperti E. et al. PD-L1 signaling on human memory CD4+ T cells induces a regulatory phenotype *PLoS Biol*. 2021;**19**:e3001199. <https://doi.org/10.1371/journal.pbio.3001199>.
44. Kazanova A, Rudd CE. Programmed cell death 1 ligand (PD-L1) on T cells generates Treg suppression from memory *PLoS Biol*. 2021;**19**:e3001272. <https://doi.org/10.1371/journal.pbio.3001272>.
45. Zhulai G, Oleinik E. Targeting regulatory T cells in anti-PD-1/PD-L1 cancer immunotherapy *Scand J Immunol*. 2022;**95**:e13129. <https://doi.org/10.1111/sji.13129>.
46. Guan X, Hu R, Choi Y. et al. Anti-TIGIT antibody improves PD-L1 blockade through myeloid and Treg cells *Nature*. 2024;**627**: 646–55. <https://doi.org/10.1038/s41586-024-07121-9>.
47. Røssevold AH, Andresen NK, Bjerre CA. et al. Atezolizumab plus anthracycline-based chemotherapy in metastatic triple-negative breast cancer: the randomized, double-blind phase 2b ALICE trial *Nat Med*. 2022;**28**:2573–83. <https://doi.org/10.1038/s41591-022-02126-1>.
48. Diskin B, Adam S, Cassini MF. et al. PD-L1 engagement on T cells promotes self-tolerance and suppression of neighboring macrophages and effector T cells in cancer *Nat Immunol*. 2020;**21**:442–54. <https://doi.org/10.1038/s41590-020-0620-x>.